ELSEVIER

Materials Science and Engineering A 420 (2006) 333–341

MATERIALS SCIENCE & ENGINEERING A

www.elsevier.com/locate/msea

Influence of pre-strain on the wear resistance of a plain carbon steel

K.K. Ray *, V. Toppo [1], S.B. Singh

Department of Metallurgical and Materials Engineering, Indian Institute of Technology, Kharagpur 721302, India

Received 17 June 2005; received in revised form 19 January 2006; accepted 27 January 2006

Abstract

Dry sliding wear behaviour of a plain carbon steel in different pre-strained conditions was examined in the severe wear regime using a pin-on-disk wear testing machine. The severe wear regime was ascertained by determining wear rates of the unstrained material at different loads. The primary experiments were supplemented by microstructural characterization, hardness assessment of specimens before and after wear tests, determination of tensile properties of the pre-strained specimens and SEM examination of the worn-out surfaces and subsurfaces. The results indicate that the wear rate of the specimens first increases up to 15% pre-strain and then decreases, while the hardness and tensile strength of the specimens monotonically increases with increased pre-strain. The mechanism of wear is observed to be subsurface cracking and delamination aided by oxidative wear. The imposed pre-strain on a specimen is considered to aggravate the nucleation of voids and microcracks resulting in degradation of wear resistance of the pre-strained specimens. The results infer that wear rates of pre-strained materials are governed by ductility or toughness apart from hardness and strength.

Keywords: Sliding wear; Steel; Pre-strain; Strain hardening exponent; Hardness; Tensile properties

1. Introduction

Structural components are often directly put into service in cold deformed condition. Cold deformation is essentially a pre-straining process, which alters dislocation substructure of metallic materials, and in turn, their deformation behaviour. There exist scattered attempts to understand structure–property relationships of cold deformed materials with emphasis on properties like strength [1,2], hardness [3], fatigue [4] and fracture [5,6]. However, till date, no organized attempt has been made to understand wear behaviour of materials in the pre-strained or cold deformed condition. It is well known that sliding wear is controlled by abrasion, adhesion and delamination [7]. The process of delamination is caused by the nucleation of voids or microcracks in a severely strained material with subsequent propagation of the cracks parallel to the surface [8]. Terheci [9] reported the existence of two mechanisms for void initiation during delamination. These are: (i) twin dislocation mechanism and (ii) void formation around hard inclusions [9]. Since both these mechanisms are governed by dislocation substructures, it is expected that pre-straining of a material will have a considerable influence on sliding wear behaviour of materials. The content of this paper is aimed to reveal the nature of such influence on the wear resistance of 0.15% carbon steel.

Hardness and tensile strength of a material generally increase with increasing pre-strain or cold work, and the rate of material removal in adhesive and abrasive wear processes is inversely proportional to hardness [10]. Thus, it is expected that pre-straining will improve the wear resistance of materials. However, Wang et al. [11] have emphasized that microstructure plays a dominant role than initial hardness of a material. These investigators have shown that pearlitic structure having Vickers hardness (Hv) of 327 kg/mm^2 had a lower wear rate than the martensitic structures having Hv of 772 kg/mm^2. Wang et al. [11] explained their observation using the phenomena of microstructural thermal stability, resistance to plastic deformation, resistance to nucleation and propagation of microcracks and thermal conductivity of the material. Subsequently, Biswas and Kailas [12] have shown that wear of titanium is significantly greater than that of copper in spite of the fact that titanium is twice as hard as copper. This was explained by the strain rate response of stress–strain diagrams, which lead to crack nucleation at different subsurface depths in materials [12]. Thus, it is difficult to predict the exact nature of the influence of pre-strain on a metallic material.

* Corresponding author. Tel.: +91 3222 283278 (O); fax: +91 3222 282280/255303.
E-mail address: kkrmt@metal.iitkgp.ernet.in (K.K. Ray).
[1] On study leave from National Institute of Foundry and Forge Technology, Ranchi 834003, India.

0921-5093/$ – see front matter © 2006 Published by Elsevier B.V.
doi:10.1016/j.msea.2006.01.093

Table 1
Chemical composition of the investigated steel (wt.%)

C	Mn	Si	P	S	Cr	Ni	Cu	Al	Ca	N_2	Fe
0.145	0.37	0.05	0.015	0.009	0.03	0.025	0.05	0.026	0.0018	70 ppm	Balance

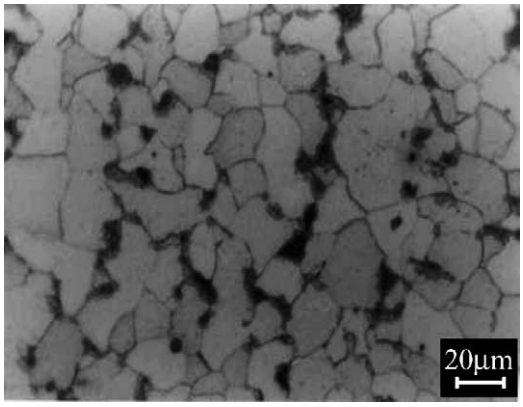

Fig. 1. Typical microstructure of the investigated 0.15%C steel.

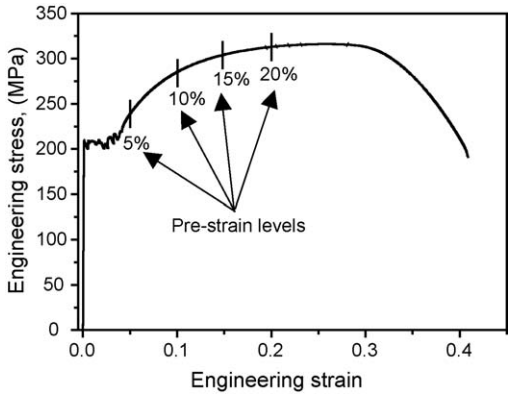

Fig. 2. Typical engineering stress–strain plot of the investigated steel, indicating the pre-strain levels at which specimen blanks were unloaded for fabricating wear specimens.

The effect of tensile pre-straining on the wear behaviour of a plain carbon steel is the major content of this paper. The selected pre-strains were limited within the uniform elongation of the steel. A series of pin-on-disk wear tests were carried out in the severe wear regime of the steel, the regime being delineated by determining the wear rates at different loads for a fixed sliding speed. The wear experiments are supplemented using studies related to tensile behaviour of the pre-strained materials, hardness measurements on specimens before and after wear tests, and SEM examinations of the worn-out surfaces and subsurfaces. The inherent aim for the overall investigation is to reveal how pre-strain affects wear resistance of a material.

2. Experimental procedures

2.1. Material and microstructure

The material used in this investigation is 0.15%C steel, which was available in the form of 13 mm diameter rods. Its chemical composition is shown in Table 1. All types of tests on this material were carried out in the annealed condition. The annealing was done at 1173 K for half an hour followed by furnace cooling. For microstructural studies, transverse sections of the rod were ground, polished up to 0.25 μm diamond finish and were then etched with 2% Nital solution. Optical microscopic examination indicated that the steel contains well-distributed mixture of ferrite and pearlite as shown in Fig. 1. The volume fraction of pearlite in the microstructure was measured by the point counting technique with the help of an image analyzer and was found to be $14.9 \pm 0.98\%$. The average ferrite grain size was determined by the linear intercept method [13] and was found to be 14.3 ± 1.8 μm. The average volume fraction of inclusion content was determined using a Japanese standard method [14] and was found to be 0.24%.

2.2. Fabrication of specimens

In order to fabricate pre-strained specimens for the wear and the tensile tests, a series of specimen blanks, approximately 150 mm in length and 8 mm in diameter, were first machined from the annealed steel rods. These were then pulled in a Shimadzu (model: AG-5000G, capacity 50 kN) testing machine at a crosshead speed of 1 mm/min at room temperature till each specimen exhibited some pre-determined extension. The pre-strain levels were selected to be 5, 10, 15 and 20%, as shown in Fig. 2. Wear pins of 4 mm diameter with 30 mm length and tensile specimens of 5 mm gage diameter with 25 mm gage length were fabricated from the pre-strained specimen blanks. The latter were fabricated following ASTM Standard E8M [15]. Similar specimens were also fabricated from the unstrained rods.

2.3. Tensile test

Tensile tests were carried out at a crosshead speed of 1 mm/min using the Shimadzu testing machine at room temperature of ≈300 K. This crosshead speed corresponds to nominal strain rate of $6.67 \times 10^{-4}\ s^{-1}$. The average 0.2% strain offset yield strength and tensile strength of the unstrained annealed steel were found to be 217 and 329 MPa, respectively, whereas the uniform and total elongations were estimated as 22.8 and 38%, respectively. The tensile properties of all the tested specimens are listed in Table 2.

2.4. Wear test

Wear experiments were performed on a pin-on-disc machine (model: Ducom TR 20) following ASTM Standard G 99-03 [16]. The disk was made of hardened En-31 steel. The initial hardness and surface roughness of the disc were Rc 62 and 0.32 μm,

Table 2
Tensile properties of the investigated specimens

Pre-strain (%)	Yield strength (MPa)	Tensile strength (MPa)	Uniform elongation (%)	Total elongation (%)
00	217 ± 9	329 ± 18	22.8 ± 3.8	38.1 ± 4.0
05	298 ± 7	357 ± 3	10.8 ± 0.1	23.4 ± 0.6
10	363 ± 4	382 ± 3	7.0 ± 0.8	19.7 ± 1.3
15	396 ± 2	405 ± 1	4.3 ± 0.5	18.4 ± 1.1
20	414 ± 11	421 ± 8	2.9 ± 0.1	16.9 ± 0.1
Test temperature	298 K			
Nominal strain rate	$6.67 \times 10^{-4}\ s^{-1}$			

respectively. The surfaces of the test pins were ground and polished up to 0.25 μm diamond finish prior to each test. Both the disk and the pin were cleaned with acetone before test, and each specimen was tested on a fresh track of the disk. All tests were carried out in air at the ambient temperature of ≈300 K and at relative humidity of ≈45% with a sliding speed of 1.2 m/s. The normal load was varied between 5 and 70 N on unstrained specimens to determine the transition load from mild to severe wear whereas a fixed load of 29 N was selected for all wear tests on the pre-strained specimens. During these tests, the frictional force was recorded using a 200 N capacity load cell whereas height loss of the pins was measured using an LVDT of 1 μm accuracy.

2.5. Hardness measurement

Microhardness measurements were carried out on the surfaces of the pins before and after the wear tests using a digital LECO (model: DM 400) microhardness tester. An indentation load of 200 gmf for loading duration of 15 s was used for these measurements. The average values of microhardness for each type of specimen were estimated from 10 readings. This is because the irregularities on the worn surfaces were large and the shape of the indentations was often found distorted [17]. For an estimation of microhardness on the worn-out surfaces, a large number of indentations were taken and the readings for normal indentations were considered following an earlier report by Goto and Amamoto [17].

2.6. SEM examination

Approximately 10 mm long samples from the end of the tested surfaces of the wear specimens were cut. A part of these samples were ground and polished in the direction normal to the test surfaces. The worn surfaces as well as their transverse sections were examined in a scanning electron microscope (model: JEOL, JSM-5800) after appropriate ultrasonic cleaning.

Table 3
Microstructural features of the selected steel

Material	SAE1015 steel
Microstructure	Ferrite–pearlite
Amount of pearlite phase	14.9 ± 0.98%
Average ferrite grain size	14.3 ± 1.8 μm
Hardness, Hv	114 ± 3.3 kg/mm^2
Volume fraction of inclusion	0.24%

Representative photographs of the surface and the subsurface (transverse direction of the specimens) of the specimens were recorded.

3. Results and discussions

3.1. Material and microstructure

The composition of the selected steel is shown in Table 1. The steel can be categorized under SAE grade 1015. The characteristics of the microstructure of the steel are discussed in Section 2.1, and these are summarized in Table 3.

3.2. Effect of pre-strain on tensile properties

The engineering stress–strain diagrams of the unstrained and the pre-strained specimens are shown in Fig. 3. The results in Fig. 3 reveal that the pre-strained specimens do not exhibit yield point phenomenon unlike the unstrained specimens. The stress–strain curves were analyzed to estimate their yield strength, tensile strength, uniform elongation and total elongation, following the suggested principles in ASTM Standard E8M [15]. The tensile properties of the

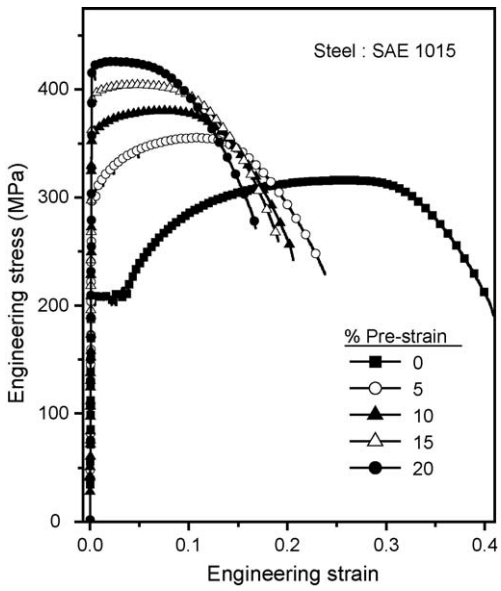

Fig. 3. Engineering stress–strain curves for specimens having varying initial pre-strains.

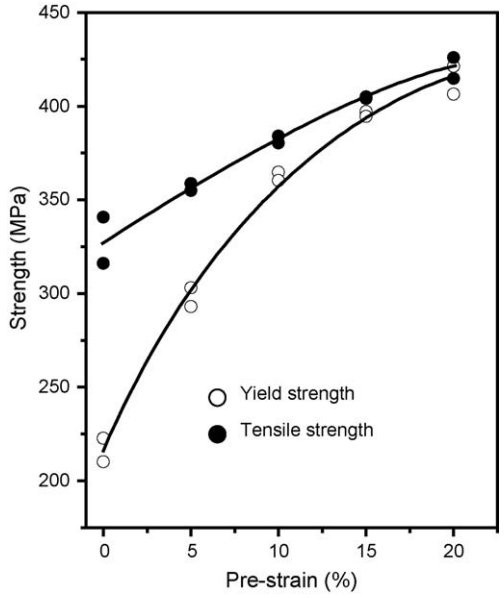

Fig. 4. Effect of pre-strain on yield and tensile strength of the investigated 0.15%C steel.

different types of specimens examined are summarized in Table 2.

The variation of yield and tensile strength with pre-strain that was imposed on the steel is shown in Fig. 4. The results in Fig. 4 reveal that both yield and tensile strength increases with increasing pre-strain; the yield to tensile strength ratio also increases with increasing pre-strain. Fig. 5 depicts the nature of variation of uniform and total elongation versus amount of imposed pre-strain. Both %uniform and %total elongation decreases with increasing pre-strain. The observations in Figs. 4 and 5 are quite similar to earlier studies on pre-strained AISI 4340 steel [18], 316 stainless steel [19] and plain C-Mn steel [20]. Thus, the recorded influence of pre-strain on tensile properties of 0.15%C steel is in agreement with similar observations made on other steels. Bassim and Bayoumi [18] demonstrated through electron microscopy of dislocation substructure that the rate of change in strength properties of 4340 steel with pre-straining has a direct correlation with the development of dislocation substructure. Following the work of Bassim and Bayoumi [18], the rapid

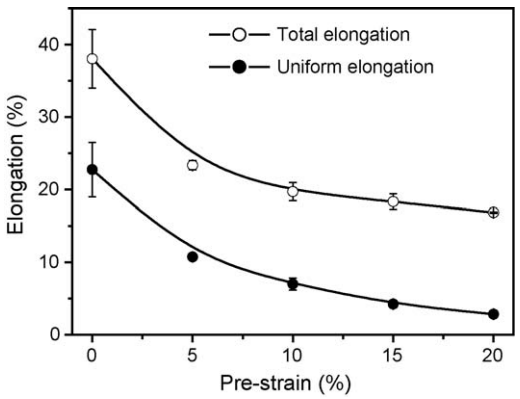

Fig. 5. Effect of pre-strain on uniform and total elongations of the investigated 0.15%C steel.

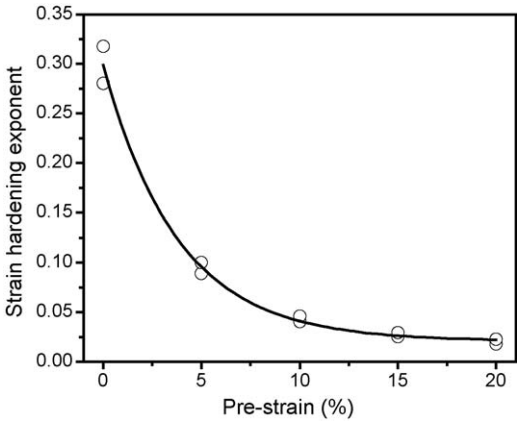

Fig. 6. Effect of pre-strain on the strain hardening exponent (n) of the investigated 0.15%C steel.

increase in yield strength with pre-strain in the selected steel is attributed to the formation of dislocation cell structure in the pre-strained specimens, which offers a higher resistance to yielding during tensile testing.

The strain hardening exponent (n) of the pre-strained specimens was determined from the slope of log (true stress) versus log (true strain) curve. The variation of 'n' with pre-strain is shown in Fig. 6. The results in Fig. 6 indicate that the magnitude of 'n' decreases with increased pre-strain for the selected

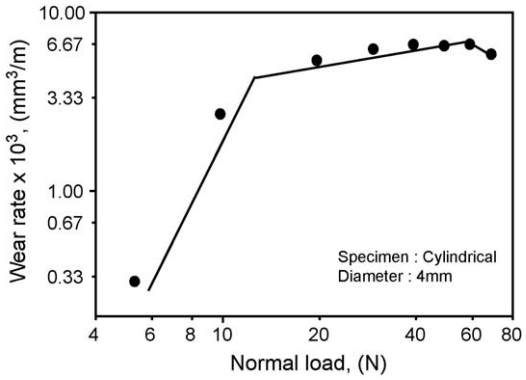

Fig. 7. Typical plot of wear rate vs. normal load for the investigated 0.15%C steel.

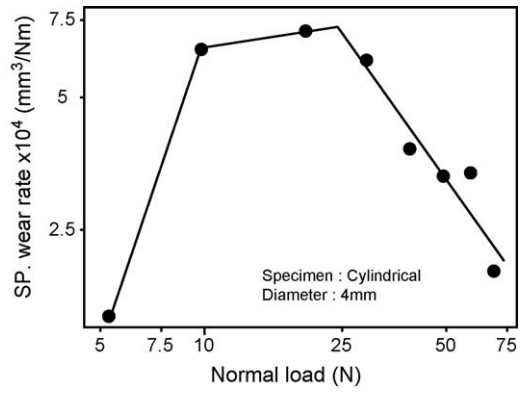

Fig. 8. Typical plot of specific wear rate vs. normal load for the investigated 0.15%C steel.

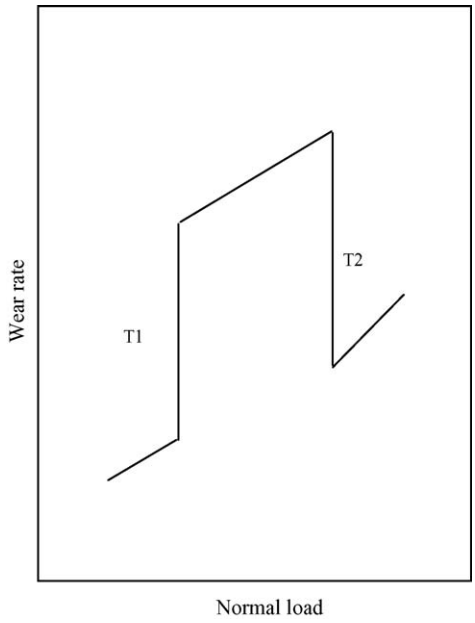

Fig. 9. Schematic diagram of wear rate vs. load showing T1 and T2 transition.

material. These results are similar to the reported variation of strain hardening exponent with pre-strain for HSLA-80 steel [5].

3.3. Estimation of transition load

The wear behaviour of the selected steel has been examined using two sequential experiments: (a) first by determining the transition load between mild to severe wear in the unstrained steel specimens and (b) second by estimating wear rate of the pre-strained specimens in the selected severe wear regime. All wear tests were carried out using pins of identical diameter of 4 mm at a sliding speed of 1.2 m/s and under identical experimental conditions of temperature, humidity and disc characteristics as described in Section 2.4. For determining the transition load for the selected material–disc system, wear tests were carried out on unstrained specimens using normal loads of 4.9, 9.8, 19.6, 29.4, 39.2, 49, 58.8 and 68.7 N. The wear rate (W) and the 'specific wear rate (W_s)' for each specimen were estimated from the last 75% of the generated data of height loss versus sliding distance (S_D). The specific wear rate is the ratio of 'wear volume' to the product of 'frictional force' and 'sliding distance'.

The variations of W and W_s versus normal load for the unstrained specimens are shown in Figs. 7 and 8 on a log–log scale. An examination of the variation of W with normal load (Fig. 7) reveals the severe wear regime of the steel. The transition loads between mild to severe wear and vice versa for the material are illustrated in Fig. 9, following the early work of Welsh [21]. Comparing the results in Fig. 7 with typical variation of wear rate with normal load in Fig. 9, it is noted that the transition between mild to severe wear for the selected steel starts at normal loads $\leq$4.9 N and severe wear regime exists above a load of 9.8 N, and the regime extends up to a load of 58.8 N. The variation of specific wear rate with normal load also indicates that the transition load is $\leq$4.9 N, the severe wear regime exists between normal loads of 9.8 and 29.4 N. On the basis of results in Figs. 7 and 8, and their comparative assessment with results shown in Fig. 9, it is concluded that severe wear regime for the selected steel is unambiguously beyond 9.8 N, and one is expected to encounter predominant severe wear around 29.4 N. On the basis of these results, a comparison of the wear behaviour of the pre-strained specimens was carried out at normal load of 29.4 N. It is concluded here that a variation of specific wear rate with normal load can be used to obtain the transition loads between severe to mild wear and vice versa.

A few reports [17,21,22] are available related to an estimation of transition loads in different steels. In 1960s Welsh [21] carried out a series of experiments on plain carbon steels having varying carbon contents so as to determine the T1 transition loads. Later, Wang et al. [22] and Goto and Amamoto [17] reported the T1 transition loads for a few more steels other than the ones reported

Table 4
Some reported transition loads between mild to severe wear in a few steels

Steels	Sliding speed (cm/s)	T1 transition load (N)	Parameters to determine T1	Testing system	Ref.
0.12%C	20	6.1	$W = W_v/S_D$	Pin-on-ring	[22]
0.34%C	1.73	27			
0.52%C	1.73	17.2		The pin and ring were of same material	
0.63%C	6.7	34.3			
0.78%C	20	115.3			
0.98%C	33	220.7			
52100 grade			$W_s = W_v/N_L S_D$	Pin-on-ring	[23]
1. Spherodized	200	20–50			
2. Pearlitic	200	20–50		Ring: WC–8% Co, Rc = 75.5	
3. Bainitic	200	50–80			
	240	20–50			
1018 grade					
1. Pearlite	200	20–50			
0.33%C	15	6.9–10.3	$W = W_V/S_D$	Pin-on-disk, disk: 0.35%C steel, Hv = 223	[17]
0.15%C	120	$\leq$4.9	$W = W_v/S_D$	Pin-on-disk, disk: En-31 steel, Rc = 62	Present

W, wear rate; W_s, specific wear rate; W_v, wear volume; W_V, total wear volume (pin + disk); N_L, normal load; S_D, sliding distance; Rc, Rockwell hardness in C scale; Hv, Vickers hardness.

by Welsh. The reported transition loads are compiled in Table 4. An examination of the results in Table 4 indicates that estimation of the transition loads has been carried out using "pin-on-ring" or using "pin-on-disk" testing systems, and the nature of the pin or the disk is different in the different reports. It is natural that the estimated transition load is a function of the testing system, sliding speed and the type of material used for fabricating the disks or the rings. Hence, it is difficult to compare the estimated magnitude of the T1 transition load for 0.15%C steel with the reported values. However, the order of the estimated transition load is considered to be comparable to the lower bound T1 value reported by Goto and Amamoto [17] for the 0.33%C steel.

3.4. Influence of pre-strain on wear behaviour

Prominent severe wear was found to occur around a normal load of 29.4 N in the unstrained steel specimens. This load was considered for all wear tests of the pre-strained specimens to achieve severe wear. The variation of wear and specific wear rate with pre-strain, for all of the tested specimens, is depicted in Figs. 10 and 11. The results in Figs. 10 and 11 indicate that both wear rate and specific wear rate increase linearly with increasing pre-strain up to 15% followed by a drop. Increased initial pre-strain implies a higher dislocation density, which in turn, with the associated substructure, facilitates the nucleation of voids and microcracks that occurs under the influence of load during wear testing. Rapid formation of voids/microcracks followed by their subsequent swift growth in the pre-strained specimens is the major reason for the enhancement of the wear rate with increased pre-strain up to 15%.

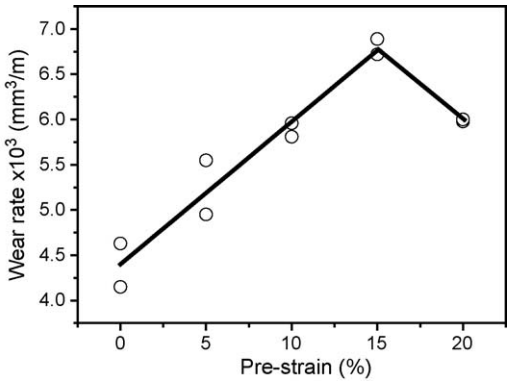

Fig. 10. Influence of pre-strain on the wear rate of the investigated 0.15%C steel.

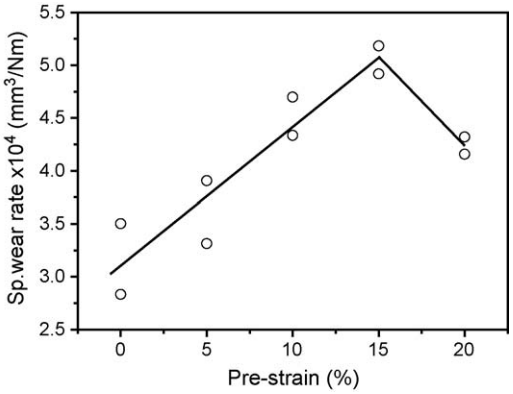

Fig. 11. Influence of pre-strain on the specific wear rate of the investigated 0.15%C steel.

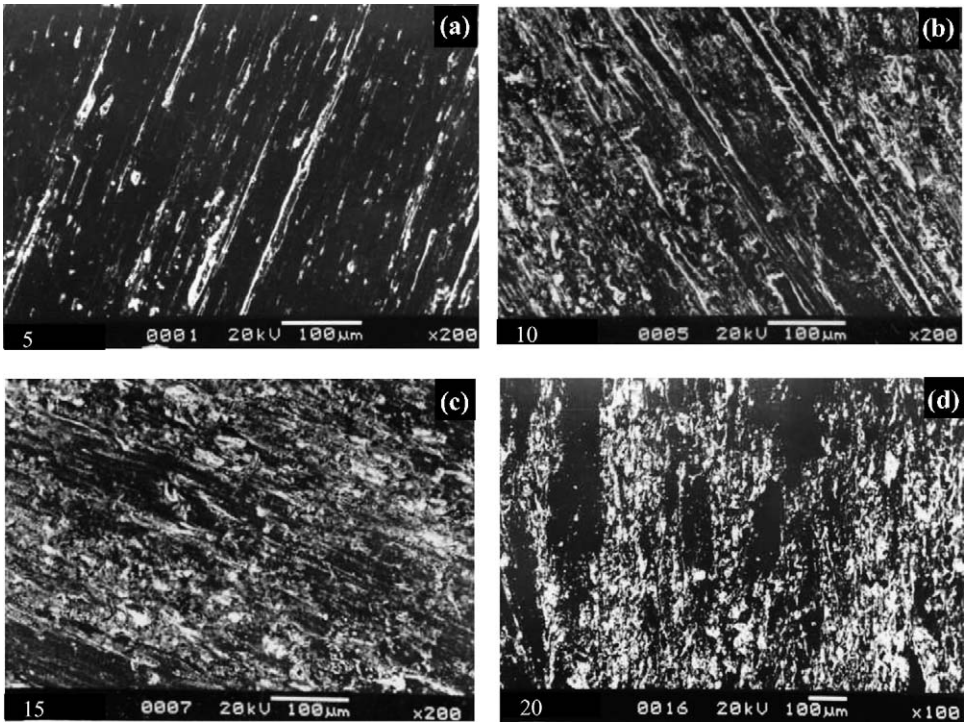

Fig. 12. SEM photographs showing worn surface of 0.15%C steel specimens at pre-strain levels (a) 5%, (b) 10%, (c) 15% and (d) 20%. Amount of grey/bright patches, indicating oxidation, increases from (a) to (c) with minor drop in (d). Accelerated subsurface cracking of the oxide layers enhances wear rate in the severe wear regime unlike that for the mild wear regime.

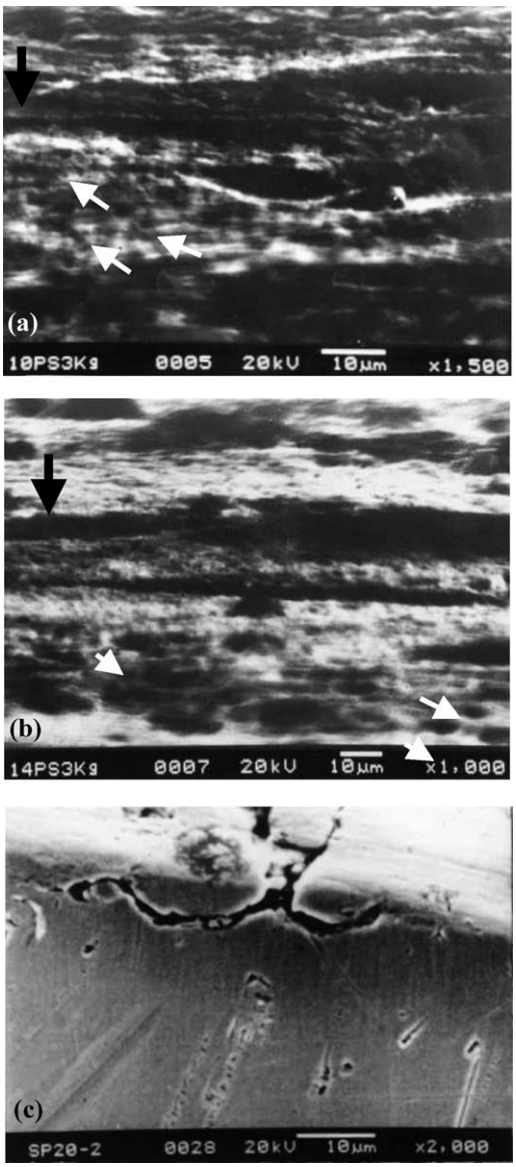

Fig. 13. SEM view of the transverse plane to the worn surfaces exhibiting: (a) elongated voids with large aspect ratio in a 10% pre-strained specimen, (b) long slender subsurface cracks in a 15% pre-strained specimen and (c) interface cracks between oxide layer and the metal in a 20% pre-strained specimen. Black arrows indicate direction of normal load whereas white arrows indicate voids or cracks.

The lower wear rate for specimens having 20% pre-strain compared to wear rates for specimens having 15% pre-strain can be attributed to two possibilities. First, the mechanism of wear in the investigated steel is due to adhesion, delamination and oxidation. These phenomena on the worn-out surfaces and subsurfaces of the pre-strained specimens are illustrated in Figs. 12 and 13. In the regime of severe wear, accelerated nucleation of voids and microcracks aggravates the process of wear by delamination. On the other hand, the wear surfaces of pre-strained specimens possessing high internal energy would be susceptible to faster oxidation. This is evident from Fig. 12. The worn-out surfaces of 5 and 10% pre-strained specimens exhibit relatively less amount of oxidation, as shown in Fig. 12(a and b), compared to those for 15 and 20% pre-strained specimens, as shown in Figs. 12(c and d). Interestingly, once oxidation takes place, the growth of the nucleated cracks is retarded. A comparative assessment of the different parts of Fig. 13 illustrates this phenomenon. Once the oxide layer is formed crack nucleation occurs at the metal–oxide interfaces as shown in Fig. 13(c). A discontinuous but an adherent oxide layer reduces the overall wear rate. However, cracking and subsequent spalling of the oxide layers cause the wear process to continue. The process of wear in the specimens having higher pre-strain is expected to be dictated by (a) the rate of nucleation of the voids/microcracks and (b) the rate of oxidation followed by its detachment or spalling from the specimen-surface. Thus, the drop in wear rate at higher pre-strain (Fig. 10) is attributed to the possible pre-dominance of the latter factor. Examination of the features on the worn surfaces did not provide any strong quantitative support to this qualitative explanation.

Second, an alternative possibility which can lead to lower wear rate in the higher pre-strained (20%) specimens is the initial nature of dislocation substructure and their interaction with the forces active during the process of wear. With increasing pre-strain, the random array of dislocations would tend to form stable dislocation cells [18]. These would not tend to impede the nucleation of microvoids and microcracks during wear but would provide a higher resistance for their growth. In addition, formation of an oxide layer would reduce the transfer of active forces to the metal substrate and aid in retarding crack growth.

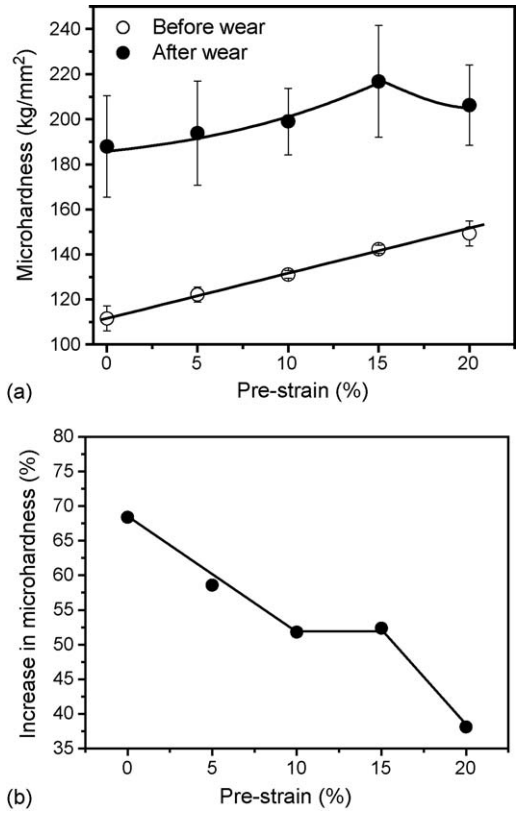

Fig. 14. Microhardness of the specimen surfaces (a) before and after the wear test and (b) percentage increase in microhardness due to wear for different pre-strained specimens.

A consequence of the above phenomena is a drop in wear rate for specimens pre-strained beyond a critical amount.

3.5. Wear vis-a-vis other mechanical properties of the pre-strained specimens

Any metallic surface subjected to wear gets work hardened. One can assess the degree of work hardening of a specimen surface by comparing its hardness estimated before and after a wear test. The degree of work hardening of the wear-tested specimens has been evaluated by this approach using microhardness tests at 200 gmf load. The obtained results are shown in Fig. 14. The initial hardness values of the pre-strained specimens (termed here as static hardness) increase with increasing pre-strain in a linear manner, as shown in Fig. 14(a). The observed increase in hardness with increased pre-strain for the specimens prior to wear test, is known to be due to strain hardening. The hardness values of the worn-out surfaces (termed as pseudo-dynamic hardness) was found to increase only up to 15% pre-strain, followed by a drop for the specimen possessing a pre-strain of 20%. The drop in pseudo-dynamic hardness for 20% pre-strained specimens is explained by the simultaneously operative wear mechanisms of delamination and 'oxidative wear'. The nature of variation of hardness of the worn-out surfaces is markedly different than that for the static hardness with pre-strain.

The degree of work hardening for a specimen due to wear can be indexed by the difference between the pseudo-dynamic and the static hardness values. This parameter has been estimated for all the specimens and its variation with specimen pre-strain is shown in Fig. 14(b). The results in Fig. 14(b) indicate that degree of work hardening during wear test of the 0.15% carbon steel decreases with increasing pre-strain up to 10%, remains almost constant between pre-strain of 10 and 15% and decreases beyond pre-strain of 15%.

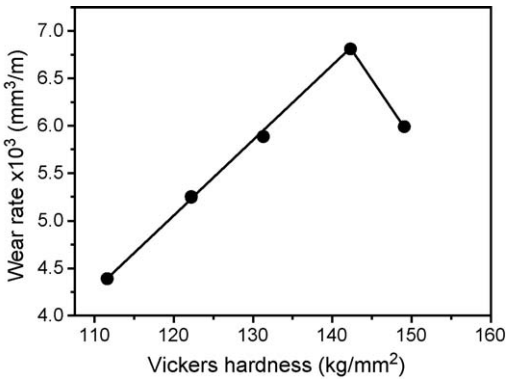

Fig. 15. Influence of initial hardness on the wear rate of the investigated pre-strained steel.

The results in Figs. 14(a) and 10 indicate that both static hardness and wear rate of the specimens investigated increase with an increasing pre-strain. A cross-plot of wear rate versus hardness, as shown Fig. 15, reveals that wear rate usually increases with increasing static hardness for the pre-strained specimens and appears to invalidate the generalized proposition rendered by Archard [10] related to the dependence of wear resistance of materials on the hardness values. Similar violation of the above-said proposition was also reported by Wang et al. [11] for steels exhibiting different microstructures and by Biswas and Kailas [12] for copper and titanium having different strain rate response. Taking into account the results of earlier reports and that of the

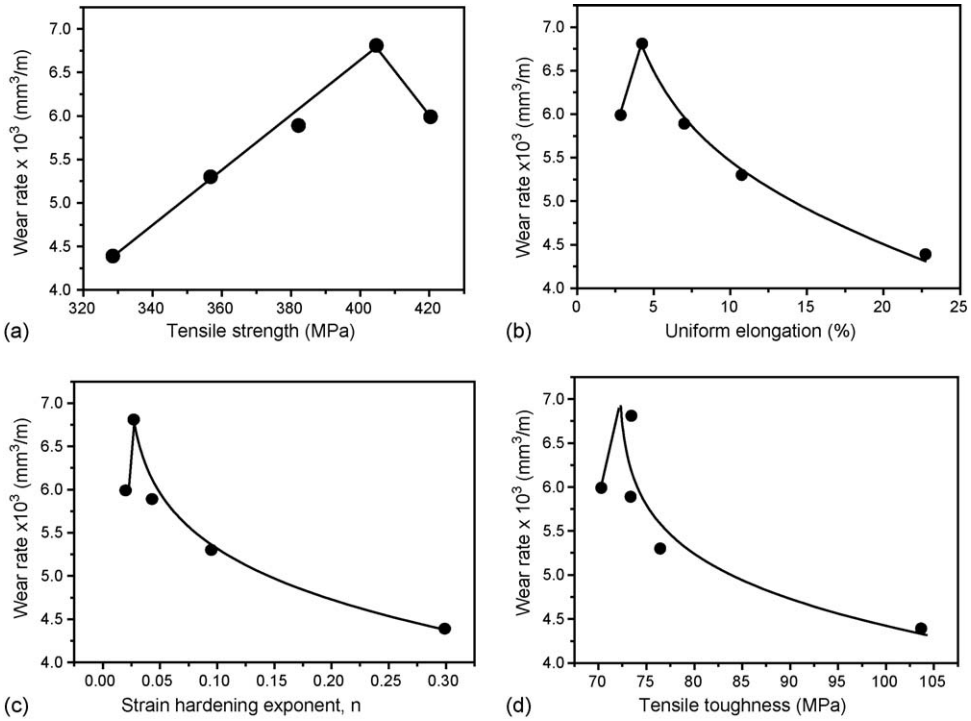

Fig. 16. Plots indicating variation of wear rate with (a) tensile strength, (b) uniform elongation, (c) strain hardening exponent and (d) tensile toughness of the investigated steel.

present investigation, it may be inferred that the microstructure or substructure dominates the wear resistance of a material rather than its hardness value.

After examining the correlation between wear rate and hardness, it becomes a natural query to examine the relationship between wear resistance and tensile properties of the pre-strained samples. The influence of pre-strain on tensile properties is discussed in Section 3.2, whereas the variation of wear rate with different tensile properties is shown in Fig. 16(a–d). Fig. 16(a) indicates that wear rate increases with increasing tensile strength in a manner similar to the variation of wear rate with hardness (Fig. 15). The nature of variation of wear rate with tensile strength of the investigated samples can be elucidated in an identical manner in explaining the variation of W with hardness using dislocation characteristics of the pre-strained steel.

The results in Fig. 16(b–d) indicate that %uniform elongation, strain hardening exponent and tensile toughness lead to an improvement in wear resistance. The parameters in the abscissa of Fig. 16(b–d) represent the tensile toughness characteristics of a material. An improvement in toughness of a material would impede the nucleation and growth of voids or microcracks resulting in the observed trend of variation of wear rate as shown in Fig. 16(b–d). In general, it is inferred that wear resistance of the investigated pre-strained steel is also governed by its toughness characteristics apart from its hardness and strength. The interrelation between wear resistance, hardness and toughness in ceramic materials has been the subject of an earlier investigation [23] by one of the authors, and this aspect will be examined in future studies to understand wear resistance of pre-strained metallic materials.

4. Conclusions

The major conclusions derived from the results of this investigation are:

1. The wear rates of the 0.15%C steel increase with increased initial pre-strain up to 15%.
2. Hardness and tensile strength of the steel increase monotonically with increasing pre-strain as per expectation. An improvement in these properties generally leads to achieving improved wear resistance of the pre-strained specimens. The results obtained are contrary to this expectation.
3. The phenomena of the ease of nucleation of voids and microcracks, and their subsequent rapid propagation are attributed to be the dominant governing factors for the deterioration of wear resistance of pre-strained (for pre-strain $\leq 15\%$) materials.
4. The overall process of wear in pre-strained specimens is governed by: (i) the ease of nucleation of voids or microcracks, which causes delamination, and (ii) oxidative wear. The drop in wear rate for specimens possessing higher pre-strain of 20% is attributed to the competitive pre-dominance of these wear processes.

References

[1] E.F. Rauch, Mater. Sci. Eng. A234–236 (1997) 653–656.
[2] S.H.M. Anijdan, H. Vahdani, Mater. Lett. 59 (2005) 1828–1830.
[3] K.F. Amouzouvi, Mater. Sci. Eng. 78 (1986) 65.
[4] D.B. Lanning, T. Nicholas, G.K. Haritos, Mech. Mater. 34 (2002) 127–134.
[5] S. Sivaprasad, S. Tarafder, V.R. Ranganath, K.K. Ray, Mater. Sci. Eng. A284 (2000) 195–201.
[6] K. Enami, Eng. Fract. Mech. 72 (2005) 1089–1105.
[7] G.M. Stachowiak, A.W. Batchelor, Engineering Tribology, Tribology Series, vol. 24, Elsevier, Amsterdam, 1993.
[8] J.R. Fleming, N.P. Suh, Wear 44 (1977) 39–56.
[9] M. Terheci, Mater. Charact. 45 (2000) 1–15.
[10] J.F. Archard, J. Appl. Phys. 24 (8) (1953) 981–988.
[11] Y. Wang, T. Lei, J. Liu, Wear 231 (1999) 12–19.
[12] S.K. Biswas, S.V. Kailas, Tribol. Int. 30 (5) (1997) 369–375.
[13] E 112-96, Annual Book of ASTM Standard, 2003.
[14] JISG-0555, Japanese Standard, 2003.
[15] E 8M-03, Annual Book of ASTM Standard, 2003.
[16] G 99-03, Annual Book of ASTM Standard, 2003.
[17] H. Goto, Y. Amamoto, Wear 254 (2003) 1256–1266.
[18] M.N. Bassim, M.R. Boyoumi, Mater. Sci. Eng. 81 (1986) 317–324.
[19] P.K. Liaw, J.D. Landes, Met. Trans. A17 (1986) 473–489.
[20] R. Sandstrom, G. Engberg, Y. Bergstrom, Met. Sci. 15 (1981) 409–412.
[21] N.C. Welsh, Proc. R. Soc. A 257 (1965) 31–70.
[22] Y. Wang, T. Lei, J. Liu, Wear 231 (1999) 1–11.
[23] A.K. Dutta, N. Narasaiah, A.B. Chattopadhyay, K.K. Ray, Mater. Manuf. Process. 17 (5) (2000) 651–670.